Appendix 1

Imaging protocol

Functional sequences and parameters

ASL: axial three-dimensional pseudo-continuous ASL (3D PCASL) of five post-label delay (PLD) was used from the skull base to the overhead. Repetition time (TR) =4,110 ms, echo time (TE) =37.78 ms, slice thickness =3.0 mm, slice number =40, slice gap =0 mm, field of view (FOV) =240 mm × 240 mm, voxel size =2.5 mm × 2.5 mm × 3.0 mm, PLD =500, 1,000, 1,500, 2,000, and 2,500 ms, scan time =7 min 12 s.

DSC: DSC PWI was performed using a gradient-echo echo-planar imaging protocol. A dynamic bolus of a standard dose of 0.1 mmol/kg gadopentetate dimeglumine (Magnevist; Beijing Beilu Pharmaceutical Co., Ltd., Beijing, China) delivered at a rate of 3 mL/s using an MRI compatible power injector [Spectris Solaris EP; Bayer (China) Co., Ltd., Shanghai, China]. The contrast bolus was followed by 20 mL of saline at the same injection rate. The imaging parameters were as follows: TR/TE =1,500/30 ms; flip angle =90°; FOV =240 mm × 240 mm; slice thickness/gap =5 mm/1.5 mm; slice number =21; matrix =128×128; 60 dynamics and total acquisition time =1 min and 38 s.

DCE: using the axial T_1WI volumetric interpolated breath-hold examination (VIBE). The T_1WI-VIBE sequence was firstly scanned at 2- and 10-degree flip angles, followed by 30 measurements dynamic enhancement scan and 15-degree flip angles. The timing of contrast injection was chosen at the end of the 5th phase. The contrast agent (gadopentetate dimeglumine, Beijing Beilu Pharmaceutical Co., Ltd.) was injected with a rate of 2.0 mL/s and a total injection of 0.1 mmol/kg. The contrast bolus was followed by 20 mL of saline at the same injection rate. The parameters: TR/TE =4.98/1.82 ms; FOV = 250 mm × 250 mm; slice thickness =2 mm; voxel size =1.4 mm × 1.4 mm × 2.0 mm; slice number =60; slice gap =0.4 mm; matrix =224×224.

MRS: two-dimensional ^{1}H multivoxel point-resolved spectroscopy was used. The ROI included regions of abnormal enhancement, perilesional edema, and contralateral/adjacent normal brain tissue, avoided the adjacent skull, hemorrhage. The parameters: TR/TE =1,700/135 ms; voxel size =10 mm × 10 mm × 15 mm; total acquisition time =6 min 53 s.

A small portion of our data were evaluated for lesion recurrence through functional MRI. When collecting functional images, i.e., ASL, DCE, structural images (3D T_1WI sequence, resolution 1 mm × 1 mm × 1 mm) are simultaneously captured. The post-processing of ASL and DCE is based on the corresponding modules in the Syngo via workstation, which register functional images with 3D structural images.

The preprocessing steps of the clustering analysis

Format conversion: apply the dcm2niix tool in the MRIcron software package to convert the raw data Dicom format into the nii.gz format and save them.

Skull stripping: the FMRIB's Software Library (FSL) was applied to remove the skull to all data through for cycle, the fail data were applied to 3D slicer for manual adjustment.

Registration: apply 3D slicer software for rigid registration, register T_2WI and ADC images to T_1WI enhanced images, and exported the format as follows: nii.gz.

Delineated ROI: the primary tumor was delineated by two radiologists (Q.F. and W.X.; with 7 and 11 years of clinical experience in brain MRI interpretation, respectively) using the ITK-SNAP 4.0 software. Both radiologists reached consensus regarding tumor delineation. Hyperintense areas were delineated on T_1WI enhanced images, including enhanced areas and internal necrosis.

Standardization: our data came from different institutions and different machine models. The python 3.9 was applied to standardize the delineated ROI data, including resampling and normalization.

https://dx.doi.org/10.21037/qims-24-1319

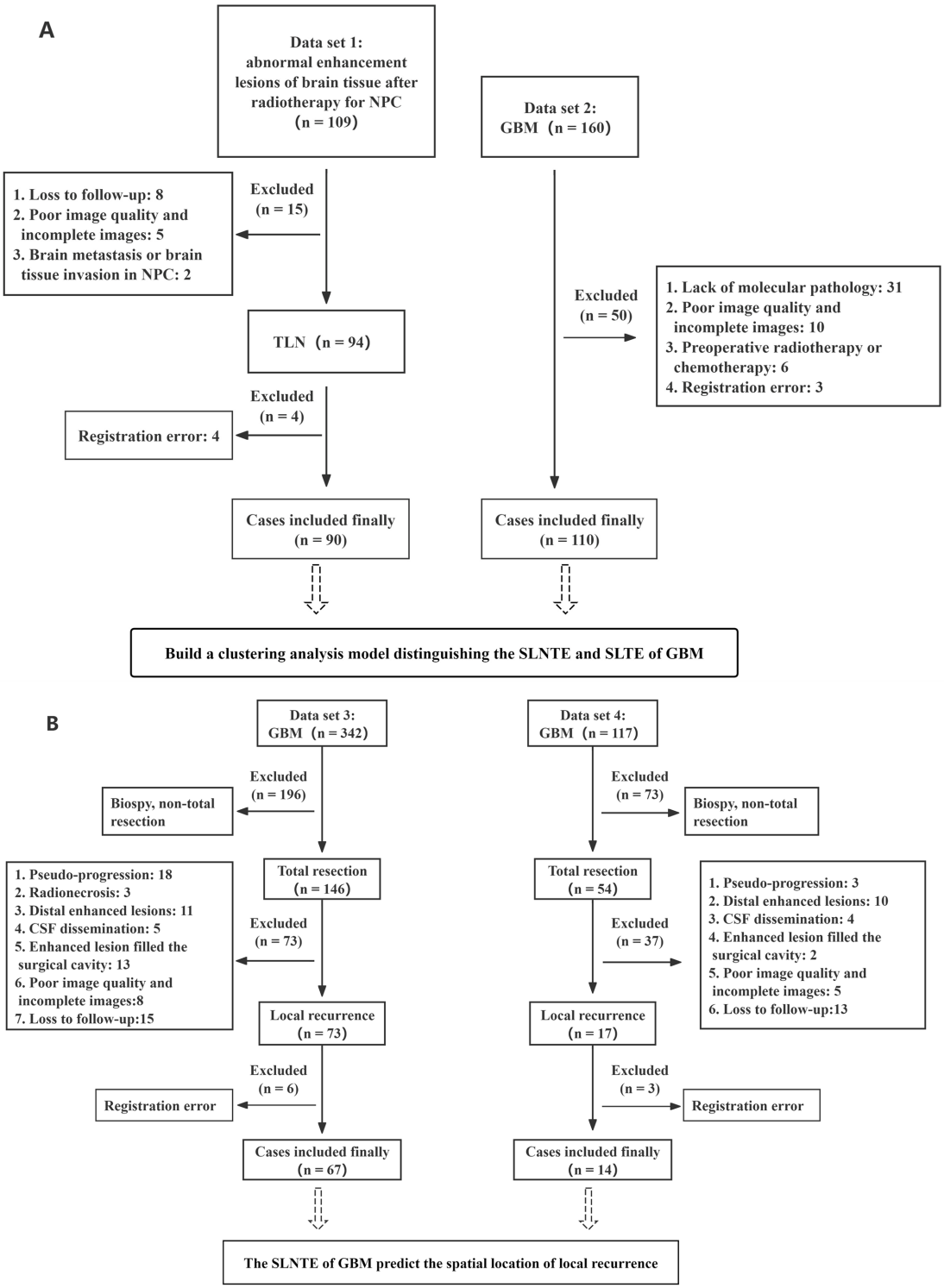

Figure S1 Flow chart of patients' inclusion and exclusion. (A) The data sets 1 and 2 came from the medical center 1. (B) The data sets 3 and 4 came from medical center 2 and center 3 respectively. Center 1, Hunan Cancer Hospital; center 2, Tianjin Huanhu Hospital; center 3, Tianjin First Central Hospital. NPC, nasopharyngeal carcinoma; GBM, glioblastoma; TLN, temporal lobe necrosis; SLNTE, spatial location of non-tumor component enhancement; SLTE, spatial location of tumor component enhancement; CSF, cerebro-spinal fluid.

https://dx.doi.org/10.21037/qims-24-1319

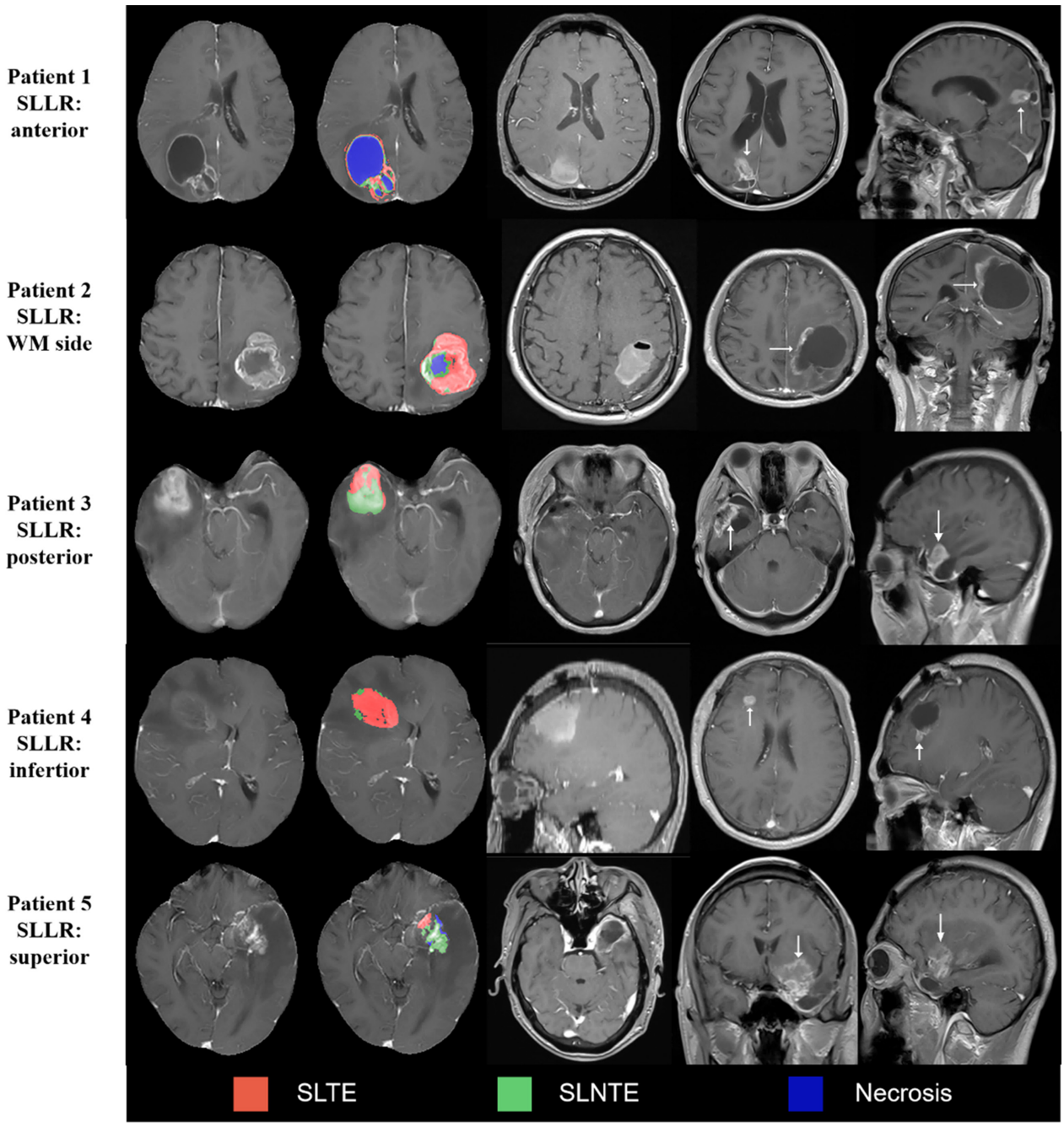

Figure S2 Examples of the SLLR for five patients with GBM. For each patient, enhanced T_1WI, clustering image, image within 3 days after surgery, and recurrent images are shown (left to right). The SLLR are indicated by the white solid arrow. SLLR, spatial location of local recurrence; WM, white matter; SLTE, spatial location of tumor enhancement; SLNTE, spatial location of non-tumor enhancement; GBM, glioblastoma; T_1WI, T_1-weighted image.

https://dx.doi.org/10.21037/qims-24-1319

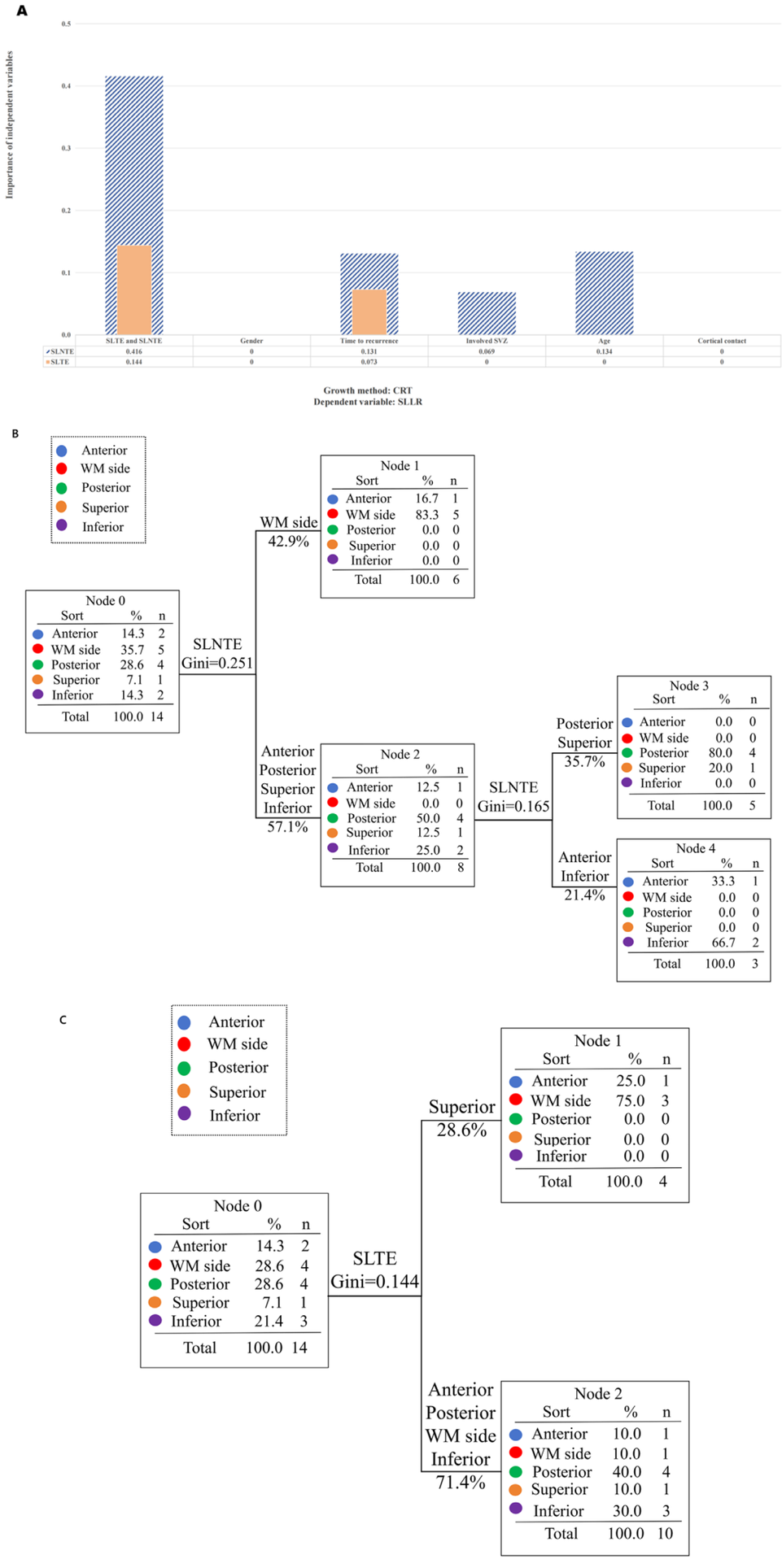

Figure S3 The importance of independent variables and the dendrograms of decision tree model in the data set 4 (center 3). The SLLR was used as the dependent variable, and the independent variables included age, sex, time to recurrence, involved SVZ, cortical contact, SLNTE, and SLTE. (A) The importance of independent variables of decision tree model based on the SLNTE and SLTE. (B,C) The dendrograms of decision tree models based on the SLNTE and SLTE, respectively. Center 3, Tianjin First Central Hospital. SLTE, spatial location of tumor component enhancement; SLNTE, spatial location of non-tumor component enhancement; SVZ, subventricular zone; WM, white matter; SLLR, spatial location of local recurrence.

https://dx.doi.org/10.21037/qims-24-1319

Table S1 MRI conventional sequences and parameters

Parameters	Data sets 1 and 2			Data set 3						Data set 4			
	T_2WI	DWI	3D-T_1WI enhancement	T_2WI	DWI	T_1WI enhancement			T_2WI	DWI	T_1WI enhancement		
MR model	Ingenia 3.0 CX			Trio Tim						Skyra			
Direction	TRA	TRA	TRA	TRA	TRA	SAG	TRA	COR	TRA	TRA	SAG	TRA	COR
TR (ms)	4,900	3,000	250	4,060	3,200	250	250	250	3,950	5,200	240	240	240
TE (ms)	100	56	2.67	93	99	2.46	2.46	2.46	99	80	2.47	2.47	2.47
Slice number	5	5	1	5	5	5	5	5	5	5	5	5	5
Thickness (mm)													
Slice gap (mm)	1.5	1.5	0	1.5	1.5	1.5	1.5	1.5	1.5	1.5	1.5	1.5	1.5
Slice number	19	19	176	21	21	17	21	20	21	21	17	21	15
Matrix	320×320	256×256	256×256	320×320	264×264	320×252	320×252	320×252	320×320	256×256	320×252	300×320	320×252
FOV (mm)	230×230	230×230	250×250	205×240	205×240	228×267	205×240	214×250	205×240	205×240	234×274	205×240	215×230

MRI, magnetic resonance imaging; T_2WI, T_2-weighted image; DWI, diffusion-weighted imaging; 3D, three-dimensional; T_1WI, T_1-weighted image; TRA, transverse plane; SAG, sagittal plane; COR, coronal plane; TR, repetition time; TE, echo time; FOV, field of vision.

https://dx.doi.org/10.21037/qims-24-1319

Table S2 Clinical and imaging characteristics of the patients with GBM

Characteristics	Data set 2 (n=110)	Data set 3 (n=67)	Data set 4 (n=14)
Age (years)	53.9±12.3	55.8±10.8	57.4±8.7
Gender (M/F)	67/43	40/27	9/5
Interval time from postoperative to radiotherapy (days)	–	29.8±11.2	32.2±6.8
Postoperative adjuvant therapy			
No	8	2	0
Radiotherapy	6	1	1
Radiotherapy and chemotherapy	60	61	13
Unknown	36	3	0
Time to recurrence (months)			
<12	–	36	7
≥12	–	31	7
Histological grade (IV grade)	All	All	All
IDH mutation (–)	All	All	All
MGMT promoter methylation (+/–)	49/61	23/44	8/6
Tumor location			
Frontal lobe (L/R)	41 (17/24)	23 (13/10)	5 (4/1)
Temporal lobe (L/R)	35 (21/14)	25 (9/16)	6(3/3)
Parietal lobe (L/R)	18 (10/8)	14 (6/8)	3 (2/1)
Occipital lobe (L/R)	15 (6/9)	3 (2/1)	NA
Cerebellum (L/R)	1 (0/1)	2 (1/1)	NA
Involved corpus callosum	47	23	4
Involved SVZ	26	11	1
Cortical contact	62	43	6

Data are presented as mean ± standard deviation or number. GBM, glioblastoma; M, male; F, female; IDH, isocitrate dehydrogenase; MGMT, O^6-methylguanine-DNA methyltransferase; L, left; R, right; SVZ, subventricular zone.

https://dx.doi.org/10.21037/qims-24-1319

Table S3 Clinical and imaging characteristics of the radiation induced TLN

Characteristics	Data set 1 (n=90)
Age (years)	49.4±10.6
Gender (M/F)	56/34
NPC clinical stage	
I	0
II	19
III	49
IV	22
NPC location	
Left	26
Right	48
Bilateral	16
Radiotherapy technology	
IMRT	33
3D-CRT	57
Radiotherapy dose (Gy)	70
Radiotherapy fractionated dose (Gy)/ frequency (f)	2/35
Radiotherapy time (days)	53 [50–58]
Site of radiation induced TLN	
Left	31
Right	45
Bilateral	14

Data are presented as mean ± standard deviation, number, or median [range]. TLN, temporal lobe necrosis; M, male; F, female; NPC, nasopharyngeal carcinoma; IMRT, intensity modulated radiation therapy; 3D-CRT, three-dimensional conformal radiation therapy.

https://dx.doi.org/10.21037/qims-24-1319

Table S4 Inter- and intra-radiologist agreement for the spatial location assessment

Data set	Spatial location	Inter		Intra	
		ICC	95% CI	ICC	95% CI
3	SLLR_ 1	0.94	0.90–0.96	0.93	0.89–0.96
	SLLR_2	0.93	0.89–0.95	0.94	0.89–0.96
	SLNTE	0.86	0.78–0.91	0.93	0.88–0.95
	SLTE	0.84	0.76–0.90	0.91	0.85–0.94
4	SLLR_ 1	0.81	0.52–0.93	0.95	0.86–0.98
	SLLR_2	0.85	0.76–0.93	0.94	0.85–0.97
	SLNTE	0.97	0.96–1.00	0.92	0.78–0.97
	SLTE	0.91	0.73–0.97	0.99	0.96–0.99

SLLR_1, the SLLR corresponding to the SLNTE; SLLR_2, the SLLR corresponding to the SLTE. ICC, intraclass correlation coefficient; CI, confidence interval; SLLR, spatial location of local recurrence; SLNTE, spatial location of non-tumor component enhancement; SLTE, spatial location of tumor component enhancement.

Table S5 The SLLR, SLNTE, and SLTE

Spatial location	Data set 3				Data set 4			
	SLLR_1	SLNTE	SLLR_2	SLTE	SLLR_1	SLNTE	SLLR_2	SLTE
Anterior	24	22	24	23	2	2	2	3
WM side	23	22	22	15	5	6	3	1
Posterior	15	14	14	13	4	2	4	4
Superior	2	2	2	2	1	2	2	1
Inferior	3	4	5	6	2	1	3	2
GM side	0	3	0	8	0	1	0	3

Data are presented as number. SLLR_1, the SLLR corresponding to the SLNTE; SLLR_2, the SLLR corresponding to the SLTE. SLLR, spatial location of local recurrence; SLNTE, spatial location of non-tumor component enhancement; SLTE, spatial location of tumor component enhancement; WM, white matter; GM, gray matter.

Table S6 Accuracy of the SLTE-based decision tree model in predicting the SLLR_2 for data set 3

Truth spatial location	Prediction					Correct percentage (%)
	Anterior	WM side	Posterior	Superior	Inferior	
Anterior	21	3	0	0	0	88
WM side	3	16	1	0	2	73
Posterior	6	1	7	0	0	50
Superior	1	1	0	0	0	0
Inferior	0	1	0	0	4	80

The accuracy of the decision tree model based on the SLTE in predicting the SLLR was 72% for data set 3. SLLR_2, the SLLR corresponding to the SLTE. SLTE, spatial location of tumor component enhancement; SLLR, spatial location of local recurrence; WM, white matter.

Table S7 Accuracy of the SLTE-based decision tree model in predicting the SLLR_2 for data set 4

Truth spatial location	Prediction					Correct percentage (%)
	Anterior	WM side	Posterior	Superior	Inferior	
Anterior	0	1	1	0	0	0
WM side	0	3	1	0	0	75
Posterior	0	0	4	0	0	100
Superior	0	0	1	0	0	0
Inferior	0	0	3	0	0	0

The accuracy of the decision tree model based on the SLTE in predicting the SLLR was 50% for data set 4. SLLR_2, the SLLR corresponding to the SLTE. SLTE, spatial location of tumor component enhancement; SLLR, spatial location of local recurrence; WM, white matter.

https://dx.doi.org/10.21037/qims-24-1319

Table S8 The diagnostic performance of the decision tree models for the data set 3

Decision tree models	Spatial location	AUC	95% CI	Sensitivity (%)	Specificity (%)
SLNTE_SLLR_1	Anterior	0.84	0.74–0.94	86	79
	WM side	0.91	0.83–0.98	91	83
	Posterior	0.89	0.78–0.99	96	73
	Superior	0.99	0.97–1.00	98	100
	Inferior	1.00	1.00–1.00	100	100
SLTE_SLLR_2	Anterior	0.89	0.80–0.97	77	88
	WM side	0.86	0.76–0.95	88	73
	Posterior	0.88	0.77–0.98	98	50
	Superior	0.73	0.49–0.98	75	50
	Inferior	0.95	0.86–1.00	97	80

SLNTE_SLLR_ 1, decision tree model for predicting the SLLR based on SLNTE; SLTE_SLLR_2, decision tree model for predicting the SLLR based on SLTE. AUC, area under the curve; CI, confidence interval; SLNTE, spatial location of non-tumor component enhancement; SLLR, spatial location of local recurrence; SLTE, spatial location of tumor component enhancement.

Table S9 The diagnostic performance of the decision tree models for the data set 4

Decision tree models	Spatial location	AUC	95% CI	Sensitivity (%)	Specificity (%)
SLNTE_SLLR_1	Anterior	0.77	0.47–1.00	83	50
	WM side	0.94	0.82–1.00	89	100
	Posterior	0.95	0.83–1.00	90	100
	Superior	0.85	0.59–1.00	69	100
	Inferior	0.95	0.85–1.00	92	100
SLTE_SLLR_2	Anterior	0.63	0.17–1.00	75	50
	WM side	0.83	0.54–1.00	90	75
	Posterior	0.70	0.42–0.97	40	100
	Superior	0.65	0.20–1.00	31	100
	Inferior	0.68	0.38–0.98	36	100

SLNTE_SLLR_ 1, decision tree model for predicting the SLLR based on SLNTE; SLTE_SLLR_2, decision tree model for predicting the SLLR based on SLTE. AUC, area under the curve; CI, confidence interval; SLNTE, spatial location of non-tumor component enhancement; SLLR, spatial location of local recurrence; SLTE, spatial location of tumor component enhancement.

https://dx.doi.org/10.21037/qims-24-1319